

***Photo-activatable fluorescent protein mEos2 displays repeated photoactivation after a long-lived dark state in the red photo-converted form***

P. Annibale<sup>1</sup>, M.Scarselli<sup>1</sup>, A. Kodiyan<sup>1</sup> and A.Radenovic<sup>1</sup>

**Supplementary Information:**

**Experimental Setup:**

The excitation setup, built on an independent optical platform, consists of three laser-diode lines, two for excitation (488nm Coherent Sapphire 488-50 and 561nm Spectra-Physics Excelsior) and one for photo-activation (405nm Coherent Cube). The excitation light is amplitude modulated and gated through an Acousto-Optical Polychromatic Tunable FilterAOM (A.A. Optoelectronics), which allows an on-off switching of each line with a rise time of 1.5  $\mu$ s. Both the activation beams are expanded (15-20X) and spatial filtered (pinhole sizes corresponding to 10  $\mu$ m and 15  $\mu$ m for the activation and excitation beam respectively). The filtered and expanded activation beam is combined to the excitation beam-path by a Semrock FF458-Di01 dichroic Mirror. The combined laser beams are focused to the back focal plane of a 1.45 NA 60X Olympus Total Internal Reflection Fluorescence objective (or of a 1.45 NA 100X Olympus Total Internal Reflection Fluorescence) by a 250 mm focal length, 25.4 mm diameter, achromatic doublet lens. Total internal reflection at the sample arises as the focused laser beams translated away from the optical axis in the back focal plane of the objective, resulting in a controllable exit angle of the beam with respect to the optical axis. In our setup the beam angle is accurately controlled by the rotation a 9.5 mm thick Fused Silica Laser Grade window(SQW-2037-UV Melles Griot) placed on a rotating goniometer. The goniometer is mounted in between the achromatic doublet and the back focal plane of the objective.

The microscope is based on the structure of an inverted Olympus model IX 81, with a camera side-port and an excitation port at the rear of the frame. Excitation and fluorescent wavelengths are separated by a Chroma T585lp dichroic mirror and a Semrock FF01-617-73 bandpass emission filter.

Single molecule fluorescence images are detected by an Andor Technology iXon+ DU-897E electron multiplying CCD camera, after a 1.2X further magnification, yielding a pixel size of 222 nm (or 133 nm). Custom developed LabView software controls the PALM acquisition sequence, triggering the CCD detector at each excitation cycle. The CCD detector in turn, has the possibility to trigger the AOM, to avoid any stray light on the CCD chip and therefore bleed-through during readout. Data is spooled to hard drive for post-processing.

### **Sample preparation:**

#### **mEos2 expression**

The mEos2FP gene is cloned into an expression cassette downstream of a T7 promoter of pRSET vector purchased from AddGene (Addgene plasmid 20341) **Figure 1 SI**.

Bacterial strain BL21(DE3) pLysS competent cells (from Stratagene) were used for protein expression that was induced by addition of IPTG (or lactose) to medium .

#### **mEos2 purification**

Next , the cells were harvested from a 100 ml culture by centrifugation and resuspended in 8 ml of lysis buffer (500 mM NaCl, 50mM NaH<sub>2</sub>PO<sub>4</sub>, pH 8).8 mg of lysozyme was added and the reaction was incubated 30 minutes on ice. The solution was sonicated on ice with a sonicator equipped with a microtip using six 10-second bursts at high intensity with a 10-second cooling period between each burst. The lysate was centrifuged at 3000 x g for 15 minutes to pellet cellular debris. The supernatant was transferred to a fresh tube.

8 ml of lysate was added to an equilibrated Invitrogen Ni-NTA Purification Column. Binding was allowed for 1 hour with gentle agitation to keep the resin suspended in the lysate solution. The resin was allowed to settle by centrifugation (800 x g) and the supernatant was carefully aspirated. The

column was washed with 8 ml of Native Wash Buffer with imidazole at low concentration (500 mM NaCl, 50 mM NaH<sub>2</sub>PO<sub>4</sub>, pH 8 and 20 mM imidazole). This last step was repeated three more times. The column was clamped in a vertical position and the cap was removed from the lower end in order to elute the protein with 12 ml native elution buffer (500 mM NaCl, 50 mM NaH<sub>2</sub>PO<sub>4</sub>, pH 8 and 250 mM imidazole). The high concentration of imidazole in the elution buffer allows the mEos2 to detach from the Ni-NTA resin.

The proteins were dialyzed in Slide-A-Lyzer cassettes with 10000 MWCO (Pierce Chemical Company, Rockford, IL) using phosphate-buffered saline (PBS) pH 7.4.

The purified mEos2 solution was diluted in an aqueous solution of Polyvinyl Alcohol (PVA)<sup>1</sup> 1% (Mowiol 4-98 Sigma Aldrich), filtered through a 0.2 um filter. Poly Acrylamide Gel (PAGE) was obtained by mixing 18% Acrylamide (Sigma) with 5% Methylenebisacrylamide (Sigma).

Samples with mEos2 concentrations ranging from 100 nM to 0.1 nM were prepared, and the PVA solution containing mEos2 was spin-coated on a glass cover-slip at 3000 RPM for 30 seconds. Glass coverslips, VWR 24 mm diameter, no. 1 thickness, were cleaned overnight in a solution obtained by mixing 125 ml of water with 25 ml of ammonium hydroxide and 25 ml of H<sub>2</sub>O<sub>2</sub> 30%. A further step based on repeated rinsing with MilliQ water, immersion in spectroscopic grade methanol, nitrogen blowing and a passage under the flame was performed.

### **Data acquisition and analysis**

Acquisition was performed with 0.1 s integration time using the frame transfer mode of the CCD chip. EM gain was used at a level yielding a photon conversion factor of 0.04 electrons/count.

561 nm excitation power, as measured in epifluorescence mode after the objective, resulted in power densities at the sample in the range of 250-1000 W/cm<sup>2</sup>. Datasets were recorded by reaching to both ends of this power range. For mEos2 we used activation powers in the in the range of 10-20 W/cm<sup>2</sup>.at

405 nm, Single molecule fluorescent traces were acquired under multiple excitation conditions see **Figure 2 SI**.

Excitation was provided either CW or through the AOTF gating (On-time=exposure time Off-time= $\sim$ 3 ms), since no significant difference was observed between the two modes of operation, the data displayed in this work were obtained with CW excitation whereas activation was either pulsed or CW. **Figure 2SI** displays single molecule kymographs recorded using multiple excitation approaches. Regardless of the excitation power of 250-1000 W/cm<sup>2</sup>, we observed reoccurring fluorescence from a non-negligible fraction of the mEos2 molecules well correlated with 405 nm activation. (**Figure 2 SI** panel a) and b)).

Many fluorophores might undergo photophysical process of fast triplet blinking due to fluorescence quenching by molecular oxygen. As reported earlier<sup>2,3</sup>, oxygen is responsible for fast triplet blinking on short time scales (typically in micro- to milliseconds)<sup>4-8</sup>. Although, triplet blinking is reported to happen at much shorter time-scales compared to the observed blinking timescales of mEos2 in our experiments (typically several s), we performed control experiments in the oxygen deprived environment prepared by flushing the samples with nitrogen (**Figure 2SI**, panel c) to exclude the above possibility. Our results, shown in (**Figure 2SI**, panel c) confirm that the observed phenomenon is not influenced by the oxygen content in the sample.

In addition 405 nm illumination was not reported to alter the short (ms range) off-times observed in another photo-activatable fluorescent proteins, such as Dronpa.

Relatively long off-time and fluorescence reoccurrence upon 405 illumination was recently reported for Dronpa protein<sup>9</sup> while shining with a relatively high frequency (4 Hz) brief activation pulses (0.04 s), superposed to a 488 nm CW excitation. We employed the proposed stroboscopic approach and we observed that this approach shortens the molecule ON time but at the same time increases remarkably number of reactivation events, as shown in **Figure 2SI**, panel d.

Furthermore it is relevant to notice that the intensity of the recorded traces, in most cases does not display any multi-step photobleaching, hinting to the fact that either dimers or oligomers are not responsible for the peculiar reactivation behavior of mEos2. Typical traces, such as the one reported in **Figure 2 SI**, panel a, yield 300-400 integrated counts per frame, with minor fluctuations.

Data analysis and scripting were performed using Wavemetrics IgorPro, whereas for single molecule identification and localization a Matlab program was employed based on the code kindly provided by Dr. Eric Betzig.

**Figure 3SI** displays the plot of the cumulative probability distribution function of the intermolecular distances of the empirical data-set against the theoretical cumulative distribution function. An approximately linear relation should be expected for the region of interest if the spatial positions of the molecules were indeed obeying a completely non-correlated spatial distribution. A convergence towards complete spatial randomness can be achieved by increasing the values of the allowed dark time  $t_d$  up to 50s, as demonstrated by increasingly linear plot of the Empirical Distribution Function  $E(t)$  vs the Theoretical One. The Theoretical Cumulative Distribution Function for points randomly spaced inside the unit circle is given by :

$$TCDF(t) = 1 + \frac{1}{\pi} \left[ 2(t^2 - 1) \arccos\left(\frac{t}{2}\right) - t \left(1 + \frac{t^2}{2}\right) * \sqrt{\left(1 - \frac{t^2}{4}\right)} \right] \quad (0.0)$$

Where  $t$  stands for the intermolecular distance.

The statistical analysis reported in the text was performed only for those samples and excitation conditions mimicking as closely as possible a real photo-activation and localization experiment in a cellular environment, either fixed or in-vivo. Following the approach reported by<sup>2</sup> histograms of on- and off-times from single molecule traces were collected. On-times

histograms were fit by a simple exponential, whereas a double exponential decay was found more appropriate to fit the off-time histograms. The longer time component in the decay could be attributed to the long lived dark state that the molecule undergoes before being resumed by 405 nm activation. **Figure 4SI** displays the residuals for the fits displayed in the text in Figure 5 a) and b).

Bi-exponential fitting of the off-times histograms, following Dickson et al., displays a marked reduction of the long off-time constant upon 405 nm irradiation.

Bi-exponential fitting of the off-times histogram on preliminary data for varying power of 561 nm excitation display, within the error, an un-modified long time constant whereas the short off-time constant appears to reduce for increasing 561 nm power.

A tentative photophysical model to explain our observations is the following.

The green form of mEos2 is converted to the red form upon 405 nm irradiation. The red form of the fluorophore deactivates upon 561 nm irradiation. However, the bi-exponential decay appearing by careful inspection of the Supporting Information of the ms by Mc-Kinney et al. hints to the presence of an additional non-fluorescent state (I) in addition to the dark state (D). According to the model originally proposed by Dickson et al. for GFP mutants, we can tentatively name this intermediate state I. The Red fluorescent state can convert to both I and D by 561 nm irradiation and, in reverse, I, with a residual absorption at 561 nm, might be responsible for the short off-time constant observed and its dependence (decrease) on 561 nm irradiation.

Irradiation by 405 nm can recover fluorescence from the dark state (D) for a limited number of times, consistently with the observed reduction of the long off-time constant upon 405 nm irradiation. D could ultimately correspond to the protonated form of the red chromophore, but our experimental strategy may lack the specificity required to demonstrate this assumption.

Under this latter respect, the behavior of mEos2 could broadly match the model reported by Dickson et al. for the GFP mutants, where 405 nm irradiation elicits photoconversion from the neutral dark state back to the green fluorescent form of the chromophore.

## References

1. Habuchi, S.; Ando, R.; Dedecker, P.; Verheijen, W.; Mizuno, H.; Miyawaki, A.; Hofkens, J. Reversible single-molecule photoswitching in the GFP-like fluorescent protein Dronpa. *Proceedings of the National Academy of Sciences of the United States of America***2005**, *102*, 9511.
2. Peterman, E. J. G.; Brasselet, S.; Moerner, W. E. The fluorescence dynamics of single molecules of green fluorescent protein: Effect of mutations, pH, and matrix. *Biophysical Journal***1999**, *76*, A445.
3. Habuchi, S.; Dedecker, P.; Hotta, J. I.; Flors, C.; Ando, R.; Mizuno, H.; Miyawaki, A.; Hofkens, J. Photo-induced protonation/deprotonation in the GFP-like fluorescent protein Dronpa: mechanism responsible for the reversible photoswitching. *Photochemical & Photobiological Sciences***2006**, *5*, 567.
4. Brown, R.; Wrachtrup, J.; Orrit, M.; Bernard, J.; Vonborczyskowski, C. Kinetics of Optically Detected Magnetic-Resonance of Single Molecules. *Journal of chemical Physics***1994**, *100*, 7182.
5. Gruber, A.; Vogel, M.; Wrachtrup, J.; Vonborczyskowski, C. Magnetic-Resonance on Single Molecules in an External Magnetic-Field - the Zeeman-Effect of a Single-Electron Spin and Determination of the Orientation of Individual Molecules. *Chem Phys Lett***1995**, *242*, 465.
6. Ha, T.; Enderle, T.; Chemla, D. S.; Selvin, P. R.; Weiss, S. Single molecule dynamics studied by polarization modulation. *Physical Review Letters***1996**, *77*, 3979.
7. Ha, T.; Enderle, T.; Chemla, D. S.; Selvin, P. R.; Weiss, S. Quantum jumps of single molecules at room temperature. *Chem Phys Lett***1997**, *271*, 1.
8. Moerner, W. E. Polymer luminescence - Those blinking single molecules. *Science***1997**, *277*, 1059.
9. Flors, C.; Hotta, J.; Uji-I, H.; Dedecker, P.; Ando, R.; Mizuno, H.; Miyawaki, A.; Hofkens, J. A stroboscopic approach for fast photoactivation-localization microscopy with Dronpa mutants. *J Am Chem Soc***2007**, *129*, 13970.

## Figures SI

### Figure 1 SI

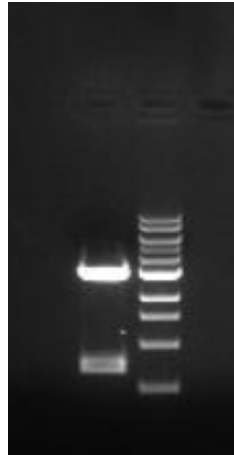


**Figure 1.SI** Gel Electrophoresis of the pRSETa plasmid containing mEos2 gene and mEos2 gene extracted with restriction enzymes BamHI and EcoRI. The lower band on the left column, corresponding to mEos2, is, as expected, around 700 bp. The right column in the 1Kb DNA ladder from New England Biolabs.

**Figure 2 SI**

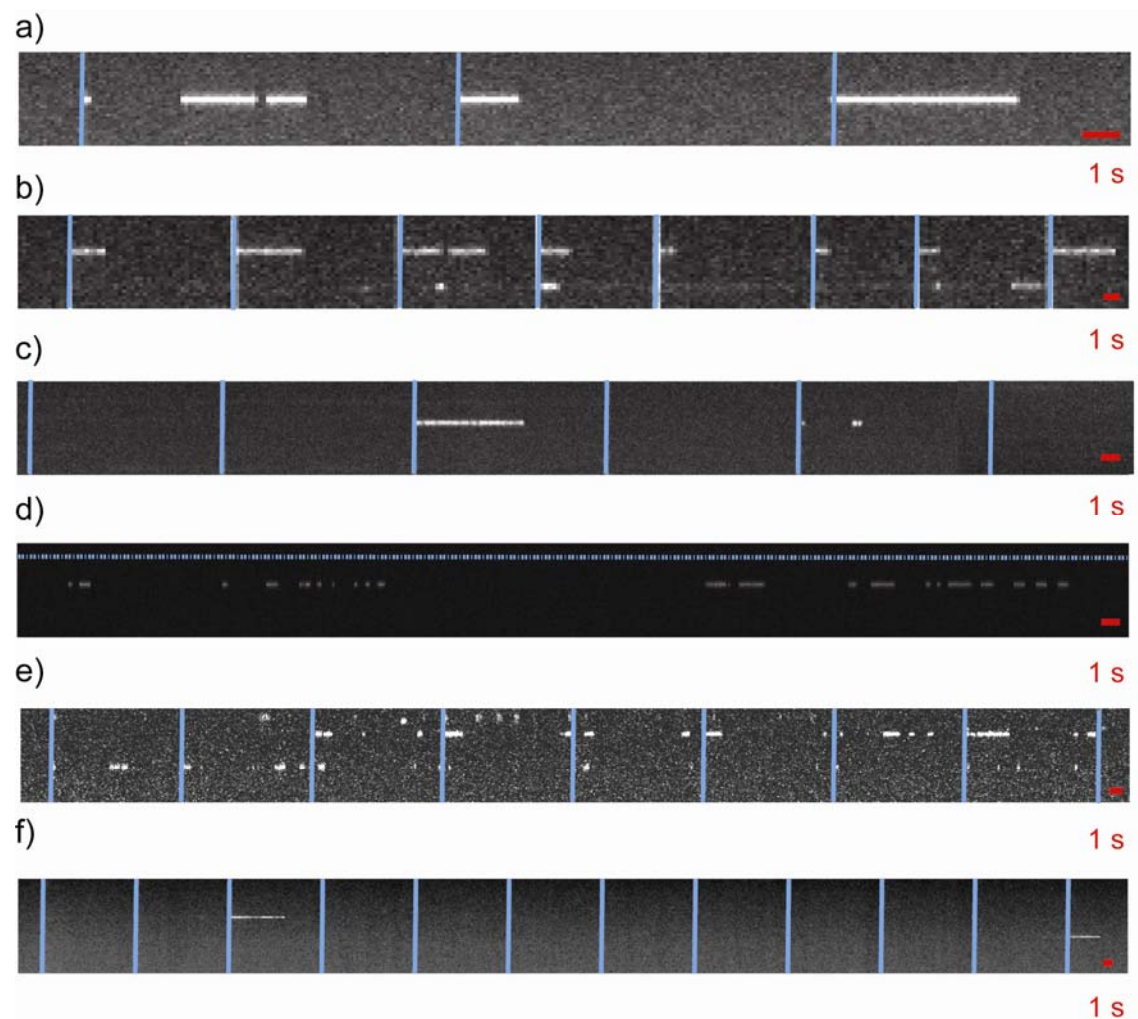


**Figure 2.SI:** Single molecule kymographs representative of the excitation approaches used in the experiments. a) 405 nm activation light ( $10 \text{ W/cm}^2$ , 0.1 s pulses) is shined on the sample in intervals of 10 s.  $1000 \text{ W/cm}^2$  excitation 561 nm wavelength is continuously supplied to the sample. b) 405 nm activation light ( $25 \text{ W/cm}^2$ , 0.2 s pulses) is shined on the sample in intervals of approximately 10 s. CW excitation is supplied at a power of a  $500 \text{ W/cm}^2$ . c) 405 nm activation light ( $25 \text{ W/cm}^2$ , 0.1 s) is shined on the sample in intervals of 10 s. CW excitation is supplied at a power of approximately  $1000 \text{ W/cm}^2$ . The sample is continuously being flushed by  $\text{N}_2$ . d) 405 nm activation light ( $25 \text{ W/cm}^2$ , 0.04 s) is shined on the sample every 250 ms. 405 activation outlined in blue in all panels. (in d not to scale e) 405 nm activation light ( $10 \text{ W/cm}^2$ , 0.1 s pulses) is shined on the sample in intervals of 10 s.  $1000$

W/cm<sup>2</sup> excitation 561 nm wavelength is continuously supplied to the sample. Panels a) d) data for mEos2 in PVA,) and in e) mEos2 is in PAGE.

f) single molecule kymograph of single molecules of PA-GFP. PA-GFP fluorescence was excited by a 488 nm laser light with a power density of approximately 500 W/cm<sup>2</sup> in TIRF mode, and imaged by the CCD camera with a 150 ms integration time. 405 nm (50 W/cm<sup>2</sup>) activation laser light was shined on the sample every 10 s without observable fluorescence reoccurrence from single PA GFP molecules.

**Figure 3 SI**

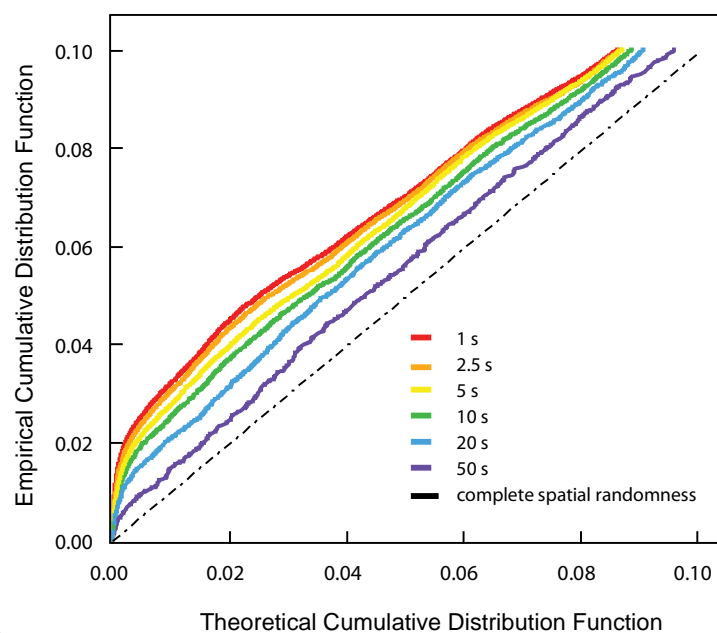


**Figure 3. SI** Measured Empirical Cumulative Distribution Function (EDF) plotted against the Theoretical Cumulative Distribution Function (TDF) for complete spatially random distributed points. Plots of the EDF vs the TDF calculated for different values of  $t_d$  and for a circular region corresponding to a circular subsection ( $R=2 \text{ \mu m}$ ) of the excitation area. The scale is enlarged to display probability values between 0 and 10%. These values are those corresponding to small intermolecular distances.

**Figure 4SI**

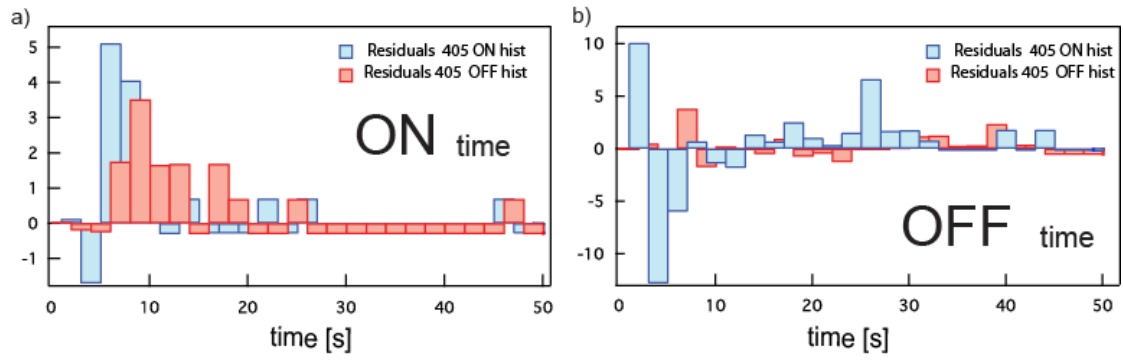


**Figure 4.SI:**Residuals for the fit displayed in Figure 5 in the text. In a) residuals from the single exponential fit to the **on-time** histogram. and in b) residuals of the double exponential fit to the **off-times** histograms.